Eur. Phys. J. D **37**, 247–253 (2006)
DOI: 10.1140/epjd/e2005-00309-0

THE EUROPEAN PHYSICAL JOURNAL D

The properties of borderlines in discontinuous conservative systems

X.-M. Wang[1,a] and Z.-J. Fang[1,2]

[1] School of Physics and Electric Information, NingXia University, Yinchuan 750021, P.R. China
[2] School of Physics, HeBei University of Technology, Tianjin 300130, P.R. China

Received 9 May 2005
Published online 16 November 2005 –

Abstract. The properties of the set of borderline images in discontinuous conservative systems are commonly investigated. The invertible system in which a stochastic web was found in 1999 is re-discussed here. The result shows that the set of images of the borderline actually forms the same stochastic web. The web has two typical local fine structures. Firstly, in some parts of the web the borderline crosses the manifold of hyperbolic points so that the chaotic diffusion is damped greatly; secondly, in other parts of phase space many holes and elliptic islands appear in the stochastic layer. This local structure shows infinite self-similarity. The noninvertible system in which the so-called chaotic quasi-attractor was found in [X.-M. Wang et al., Eur. Phys. J. D **19**, 119 (2002)] is also studied here. The numerical investigation shows that such a chaotic quasi-attractor is confined by the preceding lower order images of the borderline. The mechanism of this confinement is revealed: a forbidden zone exists that any orbit can not visit, which is the sub-phase space of one side of the first image of the borderline. Each order of the images of the forbidden zone can be qualitatively divided into two sub-phase regions: one is the so-called escaping region that provides the orbit with an escaping channel, the other is the so-called dissipative region where the contraction of phase space occurs.

PACS. 05.45.Ac Low-dimensional chaos

1 Introduction

In recent years, discontinuous conservative systems have attracted much attention [1–12]. Many strange dynamical behaviors induced by discontinuity have been observed. Some of them have attracted considerable interest. Hu et al. firstly studied a system exemplified by a particle in an infinite potential well subject to a periodic kicking force [6]. Chen et al. remodelled the system by introducing symmetrical kicks [7]. The model is described by a concatenation of two standard maps with different initial phases denoting symmetrical kicks. This map is discontinuous and invertible. The characteristic structure of phase space is a stochastic web immersed in a chaotic sea. The chaotic diffusion along this web is strongly damped when the strength of kicking force is small. A stochastic web is a common manifestation in conservative dynamic systems. This phenomenon is well known in everywhere-smooth systems, which obey the Kolmogonov-Arnold-Moser (KAM) theorem. In such systems a stochastic layer appears firstly in the neighborhood of a seperatrix as result of a non-stationary perturbation. In certain conditions, the merging of all stochastic layers in phase space can form a single network, that is, a stochastic web. This condition is often determined by a critical value of the external or driven parameter. Beyond the criticality point, the random walk of a particle along this web can take it an arbitrary distance. Thus the existence of a web means an irremovable chaotic diffusion in phase space [13]. However, in the case of reference [6] or [7], the conditions held by the KAM theorem are ruined by the discontinuity, so the mechanism for forming the stochastic web should be a fundamental problem in this system, and the cause behind why a chaotic diffusion is strongly damped is also an essential subject.

Another interesting system is a model of an electronic relaxation oscillator with over-voltage protection. Its dynamics is expressed by a discontinuous and noninvertible concatenation of two area-preserving maps. The discontinuity can induce the so-called quasi-dissipative property due to the fact that there may be two inverse images for one point, determined by the inverse mappings of the two sub-maps, respectively. In certain conditions two points located in the definition regions of the two sub-maps, respectively, may merge into one during the iteration process, which result in the collapse of phase space. The end-results of phase space contraction are the so-called "quasi-attractors". References [8,9] reported that the iterations

[a] e-mail: wxmwang@nxu.edu.cn

having started from some initial points often enter into the elliptic islands since one inverse image of a point inside the island remains inside, and the other outside. These islands may be the so-called "regular quasi-attractors". However, the end-results of phase space contraction do not exclude chaotic areas, which may be called "chaotic quasi-attractors". It had been discussed in a simplified model of the aforementioned electronic oscillator in reference [10]. The result shows that the chaotic quasi-attractor will suddenly emerge via "quasi-intermittency" when the island, or quasi-attractor, collides with the borderline and disappears completely. The investigation also shows that the set of images of the borderline forms the chaotic quasi-attractor when the number of images tends to infinity. Mira has analytically proved [14] that in certain kinds of two-dimensional piecewise noninvertible maps, the chaotic area is bounded by segments of images of the discontinuity borderline. Our recent numerical study on the system agrees with it. The sub-phase space of one side of the first image of the borderline is actually a forbidden zone that any trajectory can not visit, but that of the other side of the borderline is the sub-phase space where the chaotic quasi-attractor is located. So Mira's conclusion can be extended to this kind of discontinuous conservative system.

In this article we focus on the properties of the sets of discontinuity borderlines in both kinds of aforementioned area-preserving maps, invertible and noninvertible. For this we shall firstly present the preceding lower order images of the borderline to demonstrate how the stochastic web is gradually formed and the chaotic diffusion is confined to the web. Two types of local fine structures of the stochastic web are also presented to reveal the cause behind why the chaotic diffusion may be strongly damped. We shall then discuss the mechanism that the chaotic phase region in the noninvertible system is bounded by the segments of the preceding lower order images of the borderline. The paper is organized as follows. The discussions of the invertible system is introduced in Section 2 where two local fine structures of the stochastic web are used to resolve the problem proposed in the first paragraph. The investigations on the noninvertible system is presented in Section 3 where the forbidden zone and its images are discussed. The summary and discussion are presented in Section 4, the last section.

2 The set of images of borderline in a discontinuous and invertible system

2.1 The set of images of borderline and the stochastic web

The discontinuous and invertible model suggested in reference [7] will be discussed further to investigate more completely the properties of the discontinuity borderline. The mapping functions read

$$\begin{cases} I_{n+1} = f_{1x}(\theta_n, I_n) = I_n + K\sin(\theta_n + \alpha) \\ \theta_{n+1} = f_{1y}(\theta_n, I_n) = \theta_n + I_{n+1} \end{cases} \quad [\text{mod. } 2\pi] \quad \theta_n \in [0, \pi) \quad (1)$$

$$\begin{cases} I_{n+1} = f_{2x}(\theta_n, I_n) = I_n + K\sin(\theta_n - \alpha) \\ \theta_{n+1} = f_{2y}(\theta_n, I_n) = \theta_n + I_{n+1} \end{cases} \quad [\text{mod. } 2\pi] \quad \theta_n \in [\pi, 2\pi) \quad (2)$$

where θ and I respectively denote the position and angular momentum of the particle, K denotes the strength of the impulsive force, and α denotes the angle between the vertical direction (at which the pulse is applied) and the diameter that connects the two positions of the boundaries (hard walls).

Since the points on the borderline are non-differentiable the system will no longer have the condition required by the KAM theorem, and so all of the KAM rings that transit the border will disappear. Therefore, no local chaos exists in this system even if the perturbation is very small. It can be demonstrated by the stochastic web immersed in a chaotic sea and the boundless chaotic diffusion along this web. However, as discussed in reference [7], the diffusion coefficient, D, which defined as $D = \lim_{n\to\infty} (I_n - I_0)^2/n$ (I_0, I_n respectively denote the initial value and that after n iterations), is very small. It indicates that the chaotic diffusion is damped greatly by the web.

Many examples show that the periodic orbits often lose stability via the so-called edge collision bifurcation in dissipative systems. A point on the discontinuous borderline should be very unstable due to the fact that any small perturbation of its position in some direction will induce an infinitely large deviation. If the discontinuous point belongs to a periodic orbit, the orbit should be very unstable for similar reasons. When the discontinuous point belongs to an infinitely long iteration trajectory, the trajectory should be chaotic because it shows infinitely large deviations for a given small perturbation.

Just as Mira stated in reference [14], the phase region that is covered by the set of images of borderline is chaotic, however, it can scarcely be a chaotic attractor due to the area-preserving property of both maps (1) and (2), since their discontinuous concatenation is invertible as well. So it is easy to understand that in the iteration process the borderline is bent and split again and again to form, in the end, the stochastic web. Figure 1a shows the stochastic web when the parameters are fixed at $\alpha = 0.4, K = 0.1$. It is obtained by choosing 1000 points evenly distributed in the segment, $I \in [-0.4, 0.4]$, of borderline, $S = \{(\theta, I)\lceil_{\theta=\pi, I\in[-\pi,\pi]}\}$, and recording 3000 iterations for each of these points. By comparing carefully one can see that the stochastic web is the same of that reported in reference [7] and shown in Figure 1b. We have chosen several groups of parameters, all of the results support the same conclusion, that is, the set of images of the

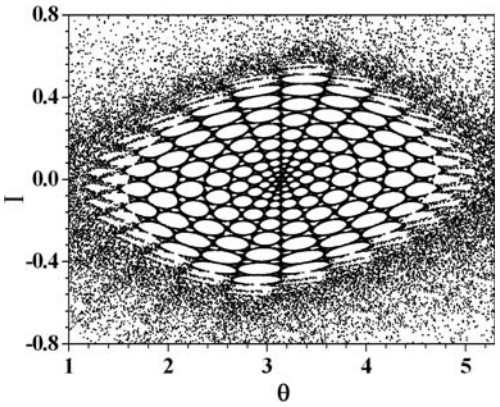

(a)

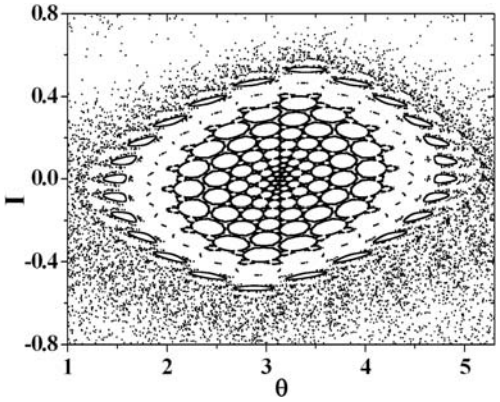

(b)

Fig. 1. Stochastic web in system (1, 2) formed by the set of discontinuous border (a) and that formed by the iterations from a point, $(\pi, 0)$. (b) The parameters and the computation methods are indicated in the text.

borderline can form a stochastic web. The first image of the borderline can be written as $S^1 = \{\theta_1, I_1\}$ that can be obtained from the equation,

$$\begin{cases} I_1 = f_{2x}(\theta_0, I_0) \\ \theta_1 = f_{2y}(\theta_0, I_0) \end{cases} \quad \forall \theta_0, I_0 \in S. \tag{3}$$

The second image of the borderline, $S^2 = \{\theta_2, I_2\}$ can be expressed as

$$\begin{cases} I_2 = f_{1x}(\theta_1, I_1) \\ \theta_2 = f_{1y}(\theta_1, I_1) \end{cases} \quad \theta_1 \in [0, \pi)$$
$$\begin{cases} I_2 = f_{2x}(\theta_1, I_1) \\ \theta_2 = f_{2y}(\theta_1, I_1) \end{cases} \quad \theta_1 \in [\pi, 2\pi) \qquad \forall \theta_1, I_1 \in S^1. \tag{4}$$

Similarly, the nth image, $S^n = \{\theta_n, I_n\}$, of the borderline can be obtained by equation,

$$\begin{cases} I_n = f_{1x}(\theta_{n-1}, I_{n-1}) \\ \theta_n = f_{1y}(\theta_{n-1}, I_{n-1}) \end{cases} \quad \theta_{n-1} \in [0, \pi)$$
$$\begin{cases} I_n = f_{2x}(\theta_{n-1}, I_{n-1}) \\ \theta_n = f_{2y}(\theta_{n-1}, I_{n-1}) \end{cases} \quad \theta_{n-1} \in [\pi, 2\pi) \qquad \forall \theta_{n-1}, I_{n-1} \in S^{n-1}. \tag{5}$$

To show the process of images of the borderline forming the stochastic web step by step, we calculated the 1st to 5th order images of the borderline analytically according to equations (3–5), and that of the 6th to 13th order numerically. We show them with the black and the dark grey curves respectively marked with the corresponding numbers of the orders in Figure 2. The magnification of Figure 1a in the neighborhood of the web center denoted with light grey is also presented. The figure obviously shows that the first image of the borderline, S^1, traverses the discontinuous border S, so the second image, S^2, is split into 2 segments, and that of third, S^3, becomes 4 segments, and so on. They often intersect one another. In the same way the images intersect in a more and more complicated manner, and finally form the stochastic web.

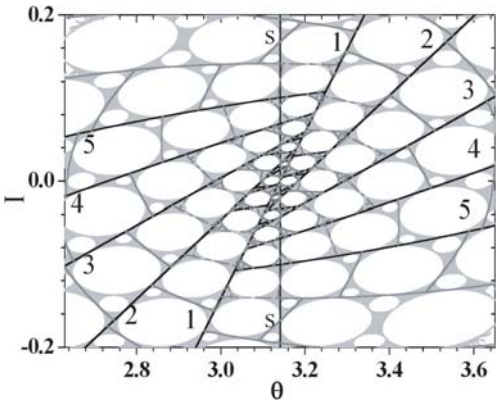

Fig. 2. Magnification of the stochastic web near its center represented by the light grey dots and the preceding 13 order images of the borderline denoted by the black and dark grey curves, respectively. The details are presented in the text.

If we consider map (1) or (2) on its own, both of them are conventional standard maps. It is well known that the standard map can be dominated by the regular motions as $K < 0.4716354$, thus the stochastic motion in the system combined by maps (1) and (2) is induced purely by the discontinuity. However, it can be expected that the dynamics of such a system partly keep the preserving rule. This may be demonstrated by many KAM regions, web holes, divided by the set of images of the borderline. In these regions the KAM theorem holds. Figure 2 also shows that each order of the images is tangent with web hole at some point. This can be predicated, as a result such images of the borderline determines the size of the web hole. In other words, they confine the chaotic motion to the web.

2.2 The fine structures of the stochastic web

To answer the problem posed in the first section concerning the stochastic web, we should consider more details that can be obtained by magnifying Figure 1. The results show that there exist some structures in the stochastic layer. The stochastic layer contains more KAM regions on a smaller scale so that the layer and the KAM regions inside it exhibit infinite self-similarity. On the same scale the stochastic web takes on two typical local fine structures.

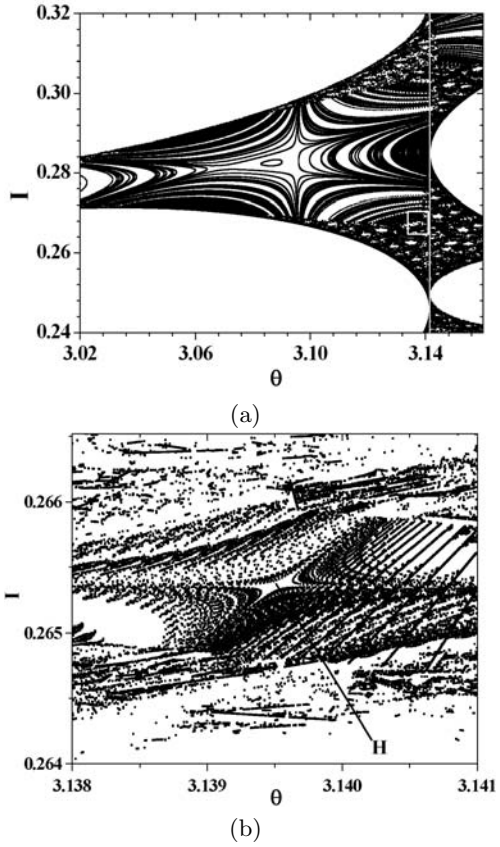

Fig. 3. (a) The magnification of Figure 1a shows the first local fine structure of the stochastic web: the discontinuity borderline crosses the manifolds of hyperbolic points in the stochastic layer. The computation is conducted by maps (1)and (2). 80000 iterations from 2000 points evenly chosen from the segment of the borderline, $\{(\theta, I)|_{\theta=\pi, I\in[0.22,0.34]}\}$, are recorded. (b) The re-magnification of the part of the phase space shown by the white square in (a) is given in the same way.

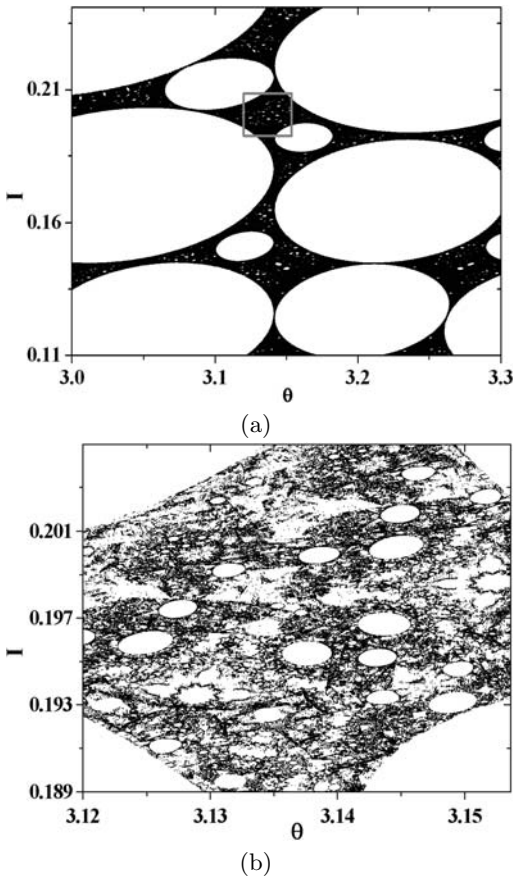

Fig. 4. (a) The magnification of Figure 1a shows the second local fine structure of the stochastic web: many web holes and corresponding islands in the stochastic layer form the local structure exhibiting infinite self-similarity. The initial points are similarly chosen evenly from the segment of the borderline, $\{(\theta, I)|_{\theta=\pi, I\in[0.264,0.267]}\}$. The computations, which are the same as those in Figure 3, are recorded. (b) The re-magnification of the part of the phase space in the grey square as shown in (a).

First, the borderline crosses the (stable or unstable) manifolds of the hyperbolic points in the stochastic layer. The borderline can chop up the KAM rings connecting the two neighboring hyperbolic points in a chain of islands. It may be important to our understanding of the structures that the Birkhoff fixed point theorem holds in some phase space. As shown in Figure 3, in phase space the appearances of the hyperbolic points often alternate with that of the elliptical ones. They may respectively form a "closed" periodic ring due to the invertible mapping, which generally is a long periodic chain surrounding a regular island chain in the stochastic layer. It should be pointed out that all of the black points in Figure 3a are computations of the points chosen evenly from the borderline with the exception of the KAM ring surrounding the little island at the center of the figure. The borderline, denoted by the grey solid line, crosses the manifold between the right two of the three hyperbolic points encircling the aforementioned central island. One example shows that the phase space of the discontinuous map can be densely filled with a countable set of discontinuity lines for the powers of the map [15], which in fact corresponds to the set of the images of the borderline (e.g., the discrete lines shown in Fig. 3b) in the current case. Accordingly the images of the borderline quite likely fall into the manifolds of hyperbolic points, and so the iterations led by these manifolds form the local stochastic web. As shown by Figure 3b, this fine structure manifests self-similarity. Figure 3b is the partial magnification of the white frame of Figure 3a. The symbol "H" denotes a hyperbolic point, and the iterations along its manifold are represented by the black dots. In conclusion, this local structure can damp down the chaotic diffusion because the iterations along the manifold, as is well known, may be very slow.

Second, as shown by Figure 4a the part nearby the center of the web often demonstrates a different structure, which shows the absence of a hyperbolic point. The iterations along the local web are not then piloted by the manifold. It is the other fine structure of the stochastic web. Two neighboring points on the discontinuity

borderline will rapidly be separated in the iteration process, thus the images of the borderline form the local structure along which the iterations should be scarcely damped. The magnification of that inside the white frame of Figure 4a (see Fig. 4b) also shows the self-similarity structure. Obviously, there exist web holes and islands inside, thus the infinite self-similarity is the basic characteristic of the stochastic web.

3 The set of images of the borderline in a discontinuous and noninvertible system

3.1 The chaotic attractor and the set of images of the borderline

The studied system can be viewed as a simplified model of the aforementioned electronic oscillator described by the discontinuous and noinvertible concatenation of De vogelaere's square map and a two-dimensional linear map [8,9], which are respectively area-preserving, i.e.,

$$\begin{cases} x_{n+1} = g_{1x}(x_n, y_n) = px_n - (1-p)x_n^2 - y_n \\ y_{n+1} = g_{1y}(x_n, y_n) = x_n - px_{n+1} + (1-p)x_{n+1}^2 \end{cases} \quad x_n \geq f \tag{6}$$

$$\begin{cases} x_{n+1} = g_{2x}(x_n, y_n) = x_n + c \\ y_{n+1} = g_{2y}(x_n, y_n) = x_n + c \end{cases} \quad x_n < f. \tag{7}$$

The backward maps of (6) and (7) can be easily written as

$$\begin{cases} x_n = g_{1x}^{-1}(x_{n+1}, y_{n+1}) \\ \quad = y_{n+1} + px_{n+1} - (1-p)x_{n+1}^2 \\ y_n = g_{1y}^{-1}(x_{n+1}, y_{n+1}) \\ \quad = -x_{n+1} + px_n - (1-p)x_n^2 \end{cases} \quad x_n \geq f \tag{8}$$

$$\begin{cases} x_n = g_{2x}^{-1}(x_{n+1}, y_{n+1}) = x_{n+1} - c \\ y_n = g_{2y}^{-1}(x_{n+1}, y_{n+1}) = y_{n+1} - c \end{cases} \quad x_n < f. \tag{9}$$

Obviously the conditions for selecting (8) or (9) to obtain the inverse image of a point (x_{n+1}, x_{n+1}) is determined by the value of x_n rather than x_{n+1}. That means that there should be two inverse images for each point (x_{n+1}, x_{n+1}), and so the system (6, 7) is noninvertible. Therefore two different points will merge into one as the iteration progress, which leads to the collapse of phase space, and is the so-called quasi-dissipative property [8–10].

The typical representation of such a quasi-dissipative property may be that quasi-attractors exist in the phase space. Here we only present the numerically obtained result in the case that the parameters are fixed where $p = -1.0069799$, $c = 0.006$, $f = -0.02$. As shown in Figure 5, the grey dots, which are 20 000 iterations recorded after ignoring the first 1000 iterations from the initial point, $(-0.035, -0.0075)$, denote the chaotic quasi-attractor. In order to illustrate that the chaotic quasi-attractor is confined by the preceding lower order images of the borderline, the black curves denoting the images from the 1st to 5th orders of the segment, $\{(x, y)|_{x=f, y\in[-0.2,0.2]}\}$,

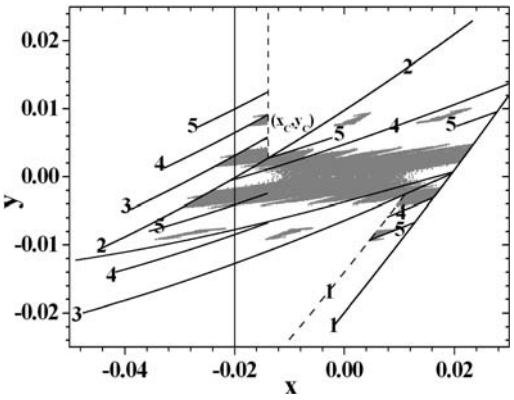

Fig. 5. Chaotic quasi-attractor and the preceding 5 images of the borderline. The details are presented in the text.

of the borderline, are drawn analytically. The curves are marked with the corresponding numbers. The analysis is obtained from the equations below which are similar to equations (3–5),

$$\begin{cases} x_1 = g_{1x}(x_0, y_0) \\ y_1 = g_{1y}(x_0, y_0) \end{cases} \quad \forall x_0, y_0 \in S, \tag{10}$$

and

$$\begin{cases} x_n = g_{1x}(x_{n-1}, y_{n-1}) \\ y_n = g_{1y}(x_{n-1}, y_{n-1}) \end{cases} \quad x_{n-1} \geq f$$
$$\begin{cases} x_n = g_{2x}(x_{n-1}, y_{n-1}) \\ y_n = g_{2y}(x_{n-1}, y_{n-1}) \end{cases} \quad x_{n-1} < f$$
$$\forall x_{n-1}, y_{n-1} \in S^{n-1} \quad n = 2, 3, \cdots, \tag{11}$$

where $S = \{(x_0, y_0)|_{x_0=f, y_0\in[-\infty,\infty]}\}$ and nth order image of the borderline, $S^n = \{x_n, y_n\}$, $n = 1, 2, \cdots$.

One can see that the borderline is split and bent again and again during the forward iteration process, and gradually confines the chaotic motion within the set of images of the borderline. Thus it can be seen that the set of the images of the borderline inevitably forms the chaotic quasi-attractor when the orders of the images tend to infinity. It is just as has been stated in reference [14]. The cause as to why the first few images can confine the chaotic quasi-attractor may be associated with some special property of the phase space outside of the set of the images of the borderline.

3.2 The forbidden zone

This special property refers to the fact that there is a forbidden zone induced by the discontinuity. For two points, (x_n^1, y_n^1) and (x_n^2, y_n^2), respectively determined by equations (8, 9) from the same point (x_{n+1}, y_{n+1}), if the inequalities, $x_n^1 < f$ and $x_n^2 \geq f$ hold, then neither (x_n^1, x_n^1) nor (x_n^2, x_n^2) is located in the definition region, so a point (x_{n+1}, y_{n+1}) has no inverse image. It follows that the phase region containing such a point is actually the forbidden zone because any point outside of this region can

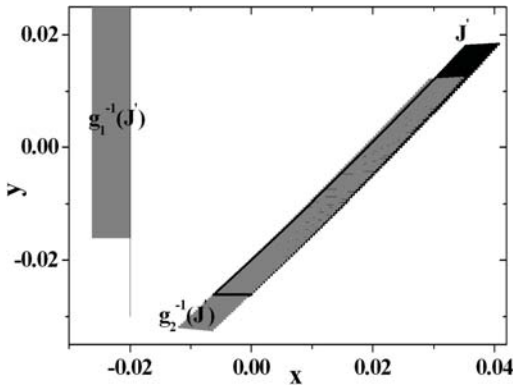

Fig. 6. This figure is schematically drawn to imply the forbidden zone by choosing its typical part J' and investigating the corresponding inverse images, $g_1^{-1}(J')$ and $g_2^{-1}(J')$.

not iterate into it. As far as the points initially located in the forbidden zone, they can not but escape out of there.

As shown in Figure 5, the first image of the borderline, S^1, denoted by the solid curve 1, is actually the right demarcation of the chaotic quasi-attractor. The sub-phase space of the right side of the first image of the borderline is the forbidden zone. We may use J to represent this phase region. As a simplified description, we take the typical representation of the forbidden zone, $J'(J' \subset J)$, the black zone nearest to the demarcation in Figure 6, to investigate its property. Please note that region J' is partly covered by its inverse image, $g_2^{-1}(J')$, shown by the grey strip (where the black horizontal line denotes the bottom edge of J'). Obviously, this inverse image of J' is located in the phase space where $x > f$, and the other, $g_1^{-1}(J')$, is located in that of $x < f$, which is also denoted by the grey strip adjacent to the discontinuity borderline. These indicate that both of the inverse images of the region J are not located in their definition regions, and as a result they do not exist. This is the reason why the first image of the borderline confines the chaotic motion. However, how can the 2nd, 3rd and the even higher order images of the borderline circumscribe the chaotic phase region? To answer this question, let's firstly discuss the 2nd image: As shown in Figure 5, after one forward iteration the forbidden zone become J^1, which is the phase region above curve 2 that represents the 2nd image of the borderline S^2. On the contrary, we can say that the region J is the inverse image of the phase region J^1, i.e. $J = g_1^{-1}(J^1)$, but its second inverse image region, $g_2^{-1}(J^1)$, only exists in the region R^1 where $x < f + c$. So the part of J^1 without the inverse image, $g_2^{-1}(J^1)$, only provides an escaping channel for the points originally located in the forbidden zone. We suggest calling it the 1st escaping region of the forbidden zone, which is denoted by the symbol, J_*^1, and given by the relation $J_*^1 = J^1 - R^1$. This region does not show the quasi-dissipative property, thus it is certain that any orbit in it is transient. Therefore, the segment of the 2nd order border image that satisfies $x \geq f + c$ can confine the chaotic motion.

The 3rd image of the borderline will now be discussed. The escaping region, J_*^1, can also be expressed as $J_*^1 = \{(x, y)|_{x \geq f+c}\} \bigcap J^1$ whose left edge is $\{(x, y)|_{x=f+c}\}$ denoted by the vertical dashed line in Figure 5. After one iteration, J_*^1 will become J^2 ($J^2 = g_1(J_*^1)$) that is between the image of the left edge of J_*^1, denoted by the dashed curve marked 1 in Figure 5, and the 3rd order image of the borderline, S^3, also shown by curve 3. Here y_c is the ordinate of the intersection point of curve 2 and the vertical dashed line, which can be easily obtained by solving the following equations.

$$\begin{cases} x' = px_0 - (1-p)x_0^2 - y \\ y' = x_0 - px' + (1-p)x'^2 \end{cases} \tag{12}$$

$$\begin{cases} x_c = px' - (1-p)x'^2 - y' \\ y_c = x' - px_c + (1-p)x_c^2 \end{cases} \tag{13}$$

$$\begin{cases} x_c = f + c \\ x_0 = f. \end{cases} \tag{14}$$

The value of y can be solved from equations (11, 12, 14), which can be substituted into equations (12, 13), and finally y_c can be obtained, i.e., $y_c \doteq 0.00269$. The sub-phase region of $J^2 = g_1(J_*^1)$ in which any point has only one inverse image should be that, $J_*^2 = \{(x, y)|_{x \geq f+c}\} \bigcap J^2$, which can be named as the 2nd order escaping region of the forbidden zone. Accordingly the segment, $x \in [f + c, g_{1x}(x_c, y_c)]$, of the 3rd order image of the borderline, denoted by solid curve 3 in Figure 5, can confine the chaotic motion.

The rest may be deduced by analogy: after one iteration the $n-1$ order escaping region of the forbidden zone can partly become that of n order, which can be generally expressed as $J_*^n = \{(x, y)|_{x \geq f+c}\} \bigcap J^n$, and the other part can become the so-called dissipative region of which there are two inverse images. One may note that the latter region actually forms a non-vacant intersection with the set of borderline images, and can finally iterate into the chaotic quasi-attractor. In fact the escaping regions differ intrinsically from the dissipative ones because the former only provide the escaping channel for the orbit originally in it, but the latter result in the phase space contraction and quasi-dissipative properties. However, they all may be the phase region where the transient orbits transit. In other words, in the dissipative region, $\{(x, y)|_{x<f+c}\}$, phase space contraction occurs, but in the region, $\{(x, y)|_{x \geq f+c}\}$, the iterations are dominated entirely by the area-preserving rule. Accordingly the iterations that are partly dissipative and partly conservative together give birth to the chaotic quasi-attractor.

4 Summary and discussion

In this paper we present some analytical and numerical investigations of the properties of the discontinuity borderline by calling attention to the characteristics shown in discontinuous systems, invertible and noninvertible. In such systems the chaotic motions are confined by the images of the borderline. In the invertible system, the confinement comes from the stochastic web formed by the set

of images of the borderline, but in the noninvertible one, the confinement is induced by the forbidden zone which is delimited by the first image of the borderline from the set of the higher order images of the borderline, as well as the chaotic quasi-attractor. The stochastic web shows two typical local fine structures: one is generated by the borderline crossing the manifolds of the hyperbolic points in the stochastic layer, which can damp down the chaotic diffusion along the web. The other has infinite self-similarity and does not have the crossing manifold so that the chaotic diffusion along this local structure is relatively rapid. In the noninvertible system, the forbidden zone means any visiting is forbidden due to any point inside this zone having no inverse image. Among the images of the forbidden zone, each order can be separated into two parts: one is the escaping region with only one inverse image, which can provide the escaping channel for the orbit originally inside the region, the other is the dissipative region with two inverse images where the phase space contraction occurs.

In other words, the sets of images of the borderlines in the invertible and noninvertible discontinuous conservative systems can be commonly regarded as generalized stochastic webs relating to the chaotic motion. For the noninvertible system, which is also the quasi-dissipative one, the chaotic quasi-attractor is the set of the borderline as the number of the images tends to infinity. This set can also form a complicated web because the borderline is split and bent again and again and intersects one another in the iteration process. The chaotic motion in the set before getting into the quasi-attractor can also be regarded as boundless chaotic diffusion along the stochastic web just as that in the invertible one. So we can say that the stochastic web is one of the basic characteristics in a discontinuous conservative system.

However, one may ask the question: what is the set of images of the borderline in a dissipative system? First, the properties of the set of images of the borderline should be the same in all kinds of discontinuous systems. Second, the set of images of the borderline is a chaotic phase region, which has been proved by many investigations.

This study is supported by the National Natural Science Foundation of China under grant No. 10565002 and Ningxia Advanced Researches Foundation of China under Grant No. 04038. The authors would like to thank Prof. Da-Ren He for the very helpful discussions and suggestions.

References

1. F. Borgonovi, G. Casati, B. Li, Phys. Rev. Lett. **77**, 4744 (1996)
2. F. Borgonovi, Phys. Rev. Lett. **80**, 4653 (1998)
3. F. Borgonovi, P. Conti, D. Rebuzz, B. Hu, B. Li, Physica D **131**, 317 (1999)
4. Y.-C. Lai, C. Grebogi, R. Blumel, I. Kan, Phys. Rev. Lett. **71**, 2212 (1993)
5. Y.-C. Lai, C. Grebogi, Phys. Rev. E **49**, 3761 (1994)
6. B. Hu, B. Li, J. Liu, Y. Gu, Phys. Rev. Lett. **82**, 4224 (1999)
7. H. Chen, J. Wang, Y. Gu, Chin. Phys. Lett, **17**, 85 (2000)
8. J. Wang, X.-L. Ding, B.-H. Wang, D.-R. He, Chin. Phys. Lett. **18**, 13 (2001)
9. J. Wang, X.-L. Ding, B. Hu, B.-H. Wang, J.-S. Mao, D.-R. He, Phys. Rev. E **64**, 026202 (2001)
10. X.-M. Wang, Y.-M. Wang, K. Zhang, X.-W. Wang, H. Chen, J.-S. Mao, D.-R. He, Eur. Phys. J. D **19**, 119 (2002)
11. Y.-M. Jiang, Y.-Q. Lu, X.-G. Chao, D.-R. He, Eur. Phys. J. D **29**, 285 (2004)
12. Y. He, Y-.M. Jiang, Y. Shen, D.-R. He, Phys. Rev. E **70**, 056213 (2004)
13. G.M. Zaslavsky, R.Z. Sagdeev, D.A. Usikov, A.A. Chernikov, *Weak chaos and quasi-regular patterns* (Cambridge University Press, Cambridge, 1991), p. 47
14. C. Mira, Inter. J. Bifur. Chaos **6**, 893 (1996)
15. Lj. Kocarev, L.O. Chua, IEEE Trans. Circuits Syst. **6**, 404 (1993)